Basophils and IgE contribute to mixed connective tissue disease development

Yasmine Lamri, Shamila Vibhushan, Emeline Pacreau, Erwan Boedec, Fanny Saidoune, Arnaud Mailleux, Bruno Crestani, Ulrich Blank, Marc Benhamou, Thomas Papo, et al.

▶ **To cite this version:**

Yasmine Lamri, Shamila Vibhushan, Emeline Pacreau, Erwan Boedec, Fanny Saidoune, et al.. Basophils and IgE contribute to mixed connective tissue disease development. Journal of Allergy and Clinical Immunology, 2021, 147 (4), pp.1478-1489.e11. 10.1016/j.jaci.2020.12.622 . hal-03405944

HAL Id: hal-03405944
https://hal.science/hal-03405944

Submitted on 24 Apr 2023

HAL is a multi-disciplinary open access archive for the deposit and dissemination of scientific research documents, whether they are published or not. The documents may come from teaching and research institutions in France or abroad, or from public or private research centers.

L'archive ouverte pluridisciplinaire **HAL**, est destinée au dépôt et à la diffusion de documents scientifiques de niveau recherche, publiés ou non, émanant des établissements d'enseignement et de recherche français ou étrangers, des laboratoires publics ou privés.

Distributed under a Creative Commons Attribution - NonCommercial 4.0 International License

Version of Record: https://www.sciencedirect.com/science/article/pii/S0091674920324088
Manuscript_e6f9332e0ef5e196af3fcc0d76f1568b

Basophils and IgE contribute to Mixed Connective Tissue Disease development

Authors: Yasmine Lamri Ph.D.[1,2], Shamila Vibhushan M.Sc.[1,2], Emeline Pacreau M.Sc.[1,2], Erwan Boedec M.Sc.[1,2], Fanny Saidoune Ph.D.[1,2], Arnaud Mailleux Ph.D.[2,3], Bruno Crestani M.D./Ph.D.[2,3,4], Ulrich Blank Ph.D.[1,2], Marc Benhamou Ph.D.[1,2], Thomas Papo M.D./Ph.D.[1,2,5], Eric Daugas M.D./Ph.D.[1,2,6], Karim Sacré M.D./Ph.D.[1,2,5] and Nicolas Charles Ph.D.[1,2]*.

[1] Université de Paris, Centre de Recherche sur l'Inflammation, INSERM UMR1149, CNRS ERL8252, Faculté de Médecine site Bichat, Paris, France.

[2] Université de Paris, Laboratoire d'Excellence Inflamex, Paris, France.

[3] Université de Paris, INSERM UMR1152, Faculté de Médecine site Bichat, Paris, France.

[4] Department of Pulmonology, Hôpital Bichat, Assistance Publique-Hôpitaux de Paris, Université de Paris, Faculté de Médecine site Bichat, DHU FIRE, Paris, France.

[5] Department of Internal Medicine, Hôpital Bichat, Assistance Publique-Hôpitaux de Paris, Université de Paris, Faculté de Médecine site Bichat, DHU FIRE, Paris, France.

[6] Department of Nephrology, Hôpital Bichat, Assistance Publique-Hôpitaux de Paris, Université de Paris, Faculté de Médecine site Bichat, DHU FIRE, Paris, France.

***Correspondence to**:

Nicolas Charles, PhD

Centre de Recherche sur l'Inflammation, INSERM UMR1149, CNRS ERL8252,

Université de Paris, Faculté de Médecine site Bichat,

16 rue Henri Huchard, 75018 Paris, France.

Phone: +33 157277306

E-mail: nicolas.charles@inserm.fr

The authors declare that they have no relevant conflict of interest.

This work was funded by ANR-11-JSV1-009-01 BASILE, ANR-15-CE17-0002 BATTLE, ANR-PIA-INFLAMEX, CNRS, AP-HP and INSERM. PhD fellowship support for Yasmine Lamri was provided by the French ministry for higher education, research and innovation (MESRI).

© 2020 published by Elsevier. This manuscript is made available under the CC BY NC user license
https://creativecommons.org/licenses/by-nc/4.0/

Key messages

- MCTD patients have activated basophils and autoreactive IgE to U1-snRNP
- Basophil depletion dampens lung pathology in a MCTD-like mouse model.
- IgE deficiency prevents the development of lung pathology in a MCTD-like mouse model.
- Basophils and IgE are promising therapeutic targets for Sharp Syndrome

Keywords

Basophil; IgE; Mixed Connective Tissue Disease; autoimmune disease pathophysiology; MCTD-like mouse model; interstitial lung disease.

Abbreviations used

AutoAb: Autoantibodies

CCR3: C-C motif chemokine Receptor 3

CCL11: C-C motif chemokine receptor Ligand 11

CIC: Circulating Immune Complexes

CXCL12: C-X-C motif chemokine receptor Ligand 12

CXCR4: C-X-C motif chemokine Receptor 4

MBP: maltose binding protein

MCTD: Mixed Connective Tissue Disease

SLE: Systemic Lupus Erythematosus

U1-snRNP: U1 small nuclear ribonucleoprotein

WT: Wild-type

CAPSULE SUMMARY

MCTD patients have activated basophils and autoreactive IgE, and both basophil depletion or IgE deficiency dampens the development of lung pathology in a MCTD-like mouse model, identifying them as putative therapeutic targets in MCTD.

ABSTRACT

Background: Mixed Connective Tissue Disease (MCTD) is a rare and complex autoimmune disease that presents mixed features with other connective tissue diseases, like systemic lupus erythematosus (SLE), systemic sclerosis and myositis. It is characterized by high levels of anti-U1-snRNP 70k autoantibodies and a high incidence of life-threatening pulmonary involvement. The pathophysiology of MCTD is not well understood and no specific treatment is yet available for the patients. Basophils and IgE play a role in the development of SLE and thus represent new therapeutic targets for SLE and other diseases involving basophils and IgE in their pathogenesis.

Objective: Investigate the role of basophils and IgE in the pathophysiology of MCTD.

Methods: Basophil activation status and the presence of autoreactive IgE were assessed in peripheral blood of a cohort of MCTD patients and in a MCTD-like mouse model. Basophil depletion and IgE-deficient animals were used to investigate the contribution of basophils and IgE in the lung pathology development of this mouse model.

Results: MCTD patients have a peripheral basopenia and activated blood basophils overexpressing C-C chemokine receptor 3 (CCR3). Autoreactive IgE raised against the main MCTD autoantigen U1-snRNP 70k were found in nearly 80% of the patients from the cohort. Basophil activation and IgE anti-U1-snRNP 70k were also observed in the MCTD-like mouse model along with basophil accumulation in lymph nodes and lungs. Basophil depletion dampened lung pathology and IgE deficiency prevented its development.

Conclusion: Basophils and IgE contribute to MCTD pathophysiology and represent new candidate therapeutic targets for MCTD patients.

INTRODUCTION

Mixed Connective Tissue Disease (MCTD) (or Sharp Syndrome) (1) is a rare systemic autoimmune disease (incidence around 2 per 100,000 adults in MN, USA) affecting mainly women (90%) (2), whose clinical manifestations can overlap with other connective tissue diseases (CTDs) such as systemic lupus erythematosus (SLE), systemic sclerosis or myositis. Over 70% of MCTD patients have pulmonary involvement that may engage vital prognosis when diagnosed (3). Serological hallmark of MCTD is the presence of high titers of autoreactive antibodies (autoAb) recognizing the 70 kDa subunit of the U1 small nuclear ribonucleoprotein (U1-snRNP 70k) along with the nearly complete absence of autoAb to double stranded DNA (dsDNA) or to Smith antigen (Sm), which are hallmarks of SLE (4). Although MCTD pathophysiology is not fully understood, post-translational modifications of U1-snRNP 70k are known to generate pathogenic neo-epitopes (5). This results in the accumulation of autoreactive B and T cells (mainly $CD4^+$) recognizing U1-snRNP 70k and subsequent autoAb production (6). Endothelial and immune cell activation via innate immune receptors, like Toll-Like Receptors (TLRs), Fc receptors and complement receptors by pathogenic complexes made of anti-U1snRNP antibodies and their antigen leads to vascular disease pathogenesis and tissue injury (7-10). Another evidence for the pathogenicity of the anti-U1snRNP antibodies comes from a mouse model that consists of immunizing mice against Human U1-snRNP and in which immunized mice develop a MCTD-like lung disease without any lupus-like features (11).

Being an autoimmune disease more frequent than MCTD, SLE has a better defined pathophysiology. In SLE, autoreactive B and T cells accumulate in secondary lymphoid organs (SLO) and lead to the production of autoAb against multiple nuclear antigens (dsDNA, RNP, Sm, Ro, La). These autoAb aggregate with autoantigens and complement factors to form circulating immune complexes (CIC) that deposit in targeted organs such as joints, skin, central nervous system and/or kidney to induce an inflammation that may lead to organ failure. SLE evolving by relapse/remission cycles, flares can be triggered by innate immune signals such as viral infection or sun exposure. These triggers, along with CIC, can activate innate immune cells such as plasmacytoid dendritic cells, monocytes,

macrophages or neutrophils to amplify autoAb production through either cytokine production (type I interferon, B cell activating factor or BAFF…) or increased autoantigen availability (neutrophil extracellular traps or NETs) (12, 13). Interestingly, the mechanistic proximity of SLE with MCTD has been exposed in animal models. Indeed, Greidinger et al. demonstrated in their mouse model of MCTD that engagement of TLR3 and/or TLR7 could trigger the development of MCTD and/or SLE, respectively (11), revealing both kinship and mechanistic differences in their respective developments.

Patients with SLE or MCTD lack specific treatments and acute phases of these diseases are contained with high dose of immunosuppressive drugs and corticosteroids (3, 4, 12, 14). Recent development of immune cell targeting immunotherapies showed limited efficacy over the standards of care (14). The clinical needs prompt further research on the pathophysiology of these CTDs to identify specific targets that may allow reducing the adverse effects of the current therapeutic modalities.

Basophils are rare innate immune cells (<1% of peripheral blood leucocytes) known for their involvement in some allergic and parasitic diseases. Recent studies evidenced their immunoregulatory role in some type 2 immunity processes, especially as primary IL-4 producers (15-17). We demonstrated their IgE- and IL-4-dependent contribution to the development of SLE, especially of lupus nephritis, in both SLE patients and murine lupus-like models (18-20). Basophils contribute to SLE pathophysiology by accumulating in secondary lymphoid organs (SLO) in a prostaglandin D2 (PGD2) and CXCL12 dependent manner (20). Indeed, basophils from SLE patients and from two distinct Lupus-like mouse models overexpress PGD2 receptors (PTGDR-1 and PTGDR-2) and CXCR4, the receptor for CXCL12 (20). Once recruited in SLO, basophils support short-lived plasma cell number and function, amplifying the peripheral titers of autoAb and CIC and their subsequent pathogenic effects (18-20).

Our previous studies on the contribution of basophils to SLE pathogenesis led to the identification of promising specific therapeutic targets in SLE, namely basophils themselves, PTGDR-1

and PTGDR-2 and IgE (18-21). The latter target showed promising effects in a human clinical trial that aimed at verifying the safety and tolerability of the anti-IgE humanized monoclonal antibody Omalizumab in SLE patients (22). Since SLE and MCTD may be related in terms of pathophysiology, we sought to investigate the putative contribution of basophils and IgE into MCTD development.

Here, we report that basophils from MCTD patients have an activated phenotype, sharing some features with basophils from SLE patients but exhibiting specific increased markers such as C-C chemokine receptor 3 (CCR3) or unchanged expression of surface markers such as CD62L. The same basophil phenotype was observed in a MCTD-like mouse model, in which activated basophils accumulated in lungs and lymph nodes. U1-snRNP immunization-induced lung disease development was dependent on both basophils and IgE demonstrating their contribution to MCTD pathophysiology in this MCTD-like mouse model. Basophils played a central effector role in maintaining the lung pro-inflammatory environment allowing interstitial lung disease and fibrosis progressions in an IgE-dependent manner. Altogether, our study identifies basophils, IgE and pathways involved in their recruitment to the lungs as candidates for the investigation of new therapeutic modalities for MCTD patients.

METHODS

Patients

All Mixed Connective Tissue Disease (MCTD) patients fulfilled the accepted diagnostic criteria without fulfillment of classification criteria for SLE, systemic sclerodermia, idiopathic inflammatory myositis or rheumatoid arthritis (2). MCTD patients and healthy control (CT) donor characteristics are shown in **Table E1** in the Online Repository. Blood samples were collected from adult patients enrolled in a prospective long term study of autoimmune diseases. The study was approved by the Comité Régional de Protection des Personnes (CRPP, Paris, France) under the reference ID-RCB 2014-A00809-38. MCTD patient samples were obtained from in- and outpatients and clinical data were harvested after approval by the Comission Nationale de l'Informatique et des Libertés (CNIL). A written informed consent was obtained from all individuals. All samples were collected in heparin blood collection tubes (Becton Dickinson) and processed within 4 hours as previously described (20).

Mice

8 weeks old female *Mcpt8*^{DTR} mice (23) on a C57BL/6J genetic background bred in our pathogen-free animal facility were kindly provided by Prof. Hajime Karasuyama (Tokyo Medical and Dental University, Tokyo, Japan). 8 weeks old female *Igh7*$^{-/-}$ mice (24) on a C57BL/6J genetic background bred in our pathogen-free animal facility were kindly provided by Prof. Hans Oettgen (Harvard Medical School, Boston, Massachusetts, USA) and Dr Juan Rivera (National Institute of Arthritis, Musculoskeletal and Skin diseases (NIAMS), NIH, Bethesda, MD, USA). Mice were maintained following the French and European guidelines and the study was approved by the local ethical committee (comité d'éthique en expérimentation animale, Faculté de Médecine Site Bichat Université Paris Diderot) and by the Department of Research of the French government under the animal study proposal number APAFIS# 14115.

Flow cytometry and antibodies

Antibodies used in both Human and murine flow cytometry data acquisition are presented in Table E2 (online repository). FACS data were collected with a LSRII-Fortessa flow cytometer using DIVA software (BD Biosciences) and analyzed with FlowJo software v10.0.7 (Treestar).

Antigen preparation

The DNA coding for U1-snRNP AA 63- 205 was optimized for E. coli production and synthesized (Eurofins genomics). The sequence was amplified by PCR and introduced in the plasmids pET28b(+) (Novagen, Millipore SAS) and pMAL-C5X (New England Biolabs) by homologous recombination (GeneArt Seamless Enzyme Mix, ThermoFisher Scientific) and transformed into E. coli Top10 (ThermoFisher Scientific). pET28b(+) allowed the production of the 70K U1-snRNP AA 63- 205 tagged by 6 histidine residues in N-terminal (His-tag). The resulting protein was used for anti-U1snRNP IgG and IgE ELISA (see below). pMAL-C5X allowed the production of the 70K U1-snRNP AA 63-205 fused to Maltose Binding Protein (MBP) in N-terminal of the fusion protein. The resulting plasmid pET28b-His-U1-snRNP and pMAL-C5X-MBP-U1-snRNP were sequenced and transformed into T7 Express Lys Y Competent E. coli (Lys Y E. coli) (New England Biolabs). Lys Y E. coli was growth at 37°C in LB-media supplemented with Kanamycin (50µg/mL) for pET28b plasmid and carbenicylin (100 µg/mL) and glucose (2 g/L) for pMAL-C5X. The productions of both recombinant proteins were induced by β-d-1-thiogalacto-pyranoside (IPTG) at 0.5 mM final during mid-exponential phase and incubated overnight at 27°C. Bacteria were pelleted and lysed by sonication. Supernatants were collected and purified on HiTrap™ TALON crude column for pET28b plasmid and MBPTrap™ HP column for pMAL-C5X plasmid (both from GE Healthcare Life Sciences). The production of MBP alone was performed with the empty vector pMAL-C5X and followed the same production protocol than pMAL-C5X-MBP-U1-snRNP. Purity of produced recombinant protein was assessed by SDS-PAGE and Coomassie blue staining and concentrations were determined by BCA protein array (ThermoFisher Scientific).

Mixed Connective Tissue Disease-like mouse model

At day 0, each mouse received subcutaneously (sc) 100 µL of a solution of complete Freund Adjuvant (CFA) emulsified vol./vol. with 50 µg of MBP-U1-snRNP (70k) fusion protein or MBP alone diluted in PBS (ThermoFisher Scientific) in the interscapular region. At day 14, mice received a sc injection of the same dose/antigen as on day 0 but emulsified in incomplete Freund adjuvant (IFA) vol./vol. Our MCTD-like induction protocol was adapted from the one from Greidinger et al.(11) and led 100 % of mice immunized against MBP-70K-U1-snRNP to develop both antibodies to these proteins and the expected MCTD-like lung disease. Mice were euthanized and analyzed at 6 weeks post-immunization as illustrated in **FIG 2A**.

Enzyme linked Immunosorbent Assays (ELISA)

Levels of IgG and IgE anti-U1-snRNP in human plasma or mice were measured by semi-quantitative ELISA on plates coated with the Human U1-snRNP protein His-tag (see antigen preparation section) at 1 µg/mL in phosphate buffered saline (PBS). The detection antibodies used were horseradish peroxidase (HRP)-conjugated sheep anti-mouse-IgG (Jackson ImmunoResearch laboratories), goat anti-mouse IgE (Bethyl laboratories), goat-anti-Human IgG (Bethyl laboratories) or goat anti-Human IgE (Bethyl laboratories) following manufacturer's instructions. Total IgE levels in patient and healthy control plasma samples were measured with the goat anti-Human IgE ELISA kit (Bethyl laboratories) following manufacturer's instructions.

Mouse sample processing

Mice were euthanized by CO_2 inhalation and processed as previously described (19, 20). For lung analysis, Broncho Alveolar Lavage (BAL) fluid was obtained by cannulating the trachea with a 20-gauge needle via an incision, and instilling 3x1 mL of Phosphate Buffered Saline (PBS). The whole lungs were lavaged and approximately 2.5 mL of BAL fluid was retrieved and centrifuged at 450 g for 5 min before resuspending the cell pellet in FACS buffer (PBS containing 1 % Bovine Serum Albumin and 0.05% NaN_3). After this step, mice were perfused with 25 mL of PBS and the whole perfused lung was isolated. The left lobe was ligated and inflated with 10% of formalin (Sigma Aldrich) during 24

hours. The lung tissues were embedded in paraffin and 5 µm sections were prepared, followed by a Masson's trichrome staining or kept for immunohistochemistry staining. The lobes of the right lung were separated for a specific use. Middle lobes were stored at -80°C in RNAprotect Tissue Reagent (Qiagen) for later RNA extraction and RT-qPCR analysis. The inferior lobe were digested with 0.2 mg/mL of Liberase TM (Roche), 0.1 mg/mL of DNAse (Sigma-Aldrich) in 1mL of RPMI 1640 containing 1% of Fetal Calf Serum (Gibco) for 1hr at 37 °C and then filtered using a cell strainer (40 µm) (Corning). The homogenate was washed in FACS buffer, centrifuge at 450 g for 5min before surface staining for flow cytometry analysis.

Immunohistochemistry

Histological sections of the lungs were dewaxed with xylene, rehydrated in graded concentrations of ethanol, and washed with PBS. Blocking of non-specific binding was realized by 30 minutes incubation in PBS containing 5% of goat serum. Antigen retrieval was performed by heating the slides 1x2minutes then 2x5minutes in Citric Buffer (10 mM, pH=6) using a microwave. Then, the anti-Rat HRP Cell & Tissue Staining Kit (R&D systems) was used following the manufacturer's instructions and with rat anti-mouse MCPT8 Antibody (clone TUG8, BioLegend) or isotype control rat IgG2a,κ (BioLegend) diluted in PBS containing 5% of goat serum to a final concentration of 1.5 µg/mL. To amplify the signal, sections were incubated with an Avidin-Biotin peroxidase complex (VECTASTAIN® ABC-HRP kit, Vector laboratories). MCPT8 localization was then visualized with a peroxidase substrate using the ImmPACT® DAB substrate diluent (Vector laboratories). Sections were then dehydrated with gradually increasing concentrations of Ethanol and then placed in xylene. Finally, the sections were counterstained with hematoxylin and coverslipped using the Eukitt® mounting medium (Kisker Biotech).

Lung pathology scores

A score of the pathology was designed to quantify inflammatory cell infiltrations in the interstitial, peribronchial and perivascular areas of the lungs. 5 µm thin sections were stained with Masson's

trichrome. Stained slides were scanned with an Aperio CS2 digital pathology slide scanner (Leica) and analyzed with the Aperio ImageScope software v.12.3 (Leica). For each area, 10 fields per lung as depicted in Figure 2 were scored from 0 to 3 as follows: 0: absence of infiltrate; 1: low number of infiltrating cells (5-20 % of the observed area); 2: moderate number of infiltrating cells (25-50 % of the observed area); 3: high number of infiltrating cells (more than 50 % of the observed area)). The mean score per affected area was calculated and multiplied by the proportion of fields showing affected areas.

Quantitative RT-PCR

RNA extraction was performed as described in the manufacturer's protocol (RNeasy Mini kit, Qiagen). cDNA was synthesized with iScript cDNA Synthesis Kit (Bio-Rad). Quantitative PCR was performed with SsoAdvanced SYBR green reaction mix (Bio-Rad) using the following KiCqStart™ Primers pairs (purchased from Sigma-Aldrich): M_Il4_1; M_Ccl11_1; M_Ifng_1; M_Actb_1; M_Col3a1_2; M_Col1a1_2 and M_Cxcl12_1 to respectively measure IL-4, CCL11, IFNγ, β-actin, COL3A1, COL1A1 and CXCL12 mRNA expression levels. Quantitative PCR was performed on the CFX96 Touch Real Time PCR Detection System (Bio-Rad) and following amplification, Ct values were obtained using the CFX Manager™ software 2.1 (Bio-Rad).

In-vivo basophil depletion

Female *Mcpt8*^{DTR} mice (with the C57BL/6 genetic background) received four intraperitoneal injections of 1 µg of diphteria toxin (D05664; Sigma-Aldrich) (or the corresponding vehicle, PBS) in 100 µL of PBS 10, 9, 4 and 1 days before sacrifice as illustrated in **FIG 2A**.

Statistics

Distribution was assessed with D'Agostino-Pearson omnibus normality test or Kolmogorov-Smirnov test, depending on sample size. When more than 2 groups were compared, one-way analysis of variance (ANOVA) tests were conducted before the indicated post-tests. All tests run were two-tailed. Data are represented either as mean ± s.e.m. or as median and interquartile ranges with

whiskers representing 5-95 percentiles and the mean presented as a '+' symbol. In all figures, comparison to control group is shown above each bar and to the corresponding bars when indicated. Statistics were performed with GraphPad Prism version 6.0 software. NS: not significant, *: $P<0.05$, **: $P<0.01$, ***: $P<0.001$, ****: $P<0.0001$. A.U.: arbitrary units.

RESULTS

MCTD patients have activated basophils and autoreactive IgE raised against U1-snRNP

Basophils contribute to SLE pathogenesis during which they show an activated phenotype, as we previously described (18, 20). MCTD having a SLE-related pathophysiology, we analyzed the phenotype of peripheral blood basophils from a small prospective cohort of MCTD patients and compared these basophil phenotypes to healthy volunteers (CT) matched for sex and age, whose characteristics are described in **Table E1** (in the Online Repository). The flow cytometry gating strategy is described in **FIG E1A** (see the Online Repository). MCTD patient basophils showed an activated phenotype (**FIG 1A-G**). Interestingly, the global activation profile of basophils from MCTD patients differed to some extent from that of SLE patients (18, 20). Indeed, like SLE patients, MCTD patients showed a peripheral basopenia (**FIG 1A-B**), an increased expression of the activation marker CD203c and of the CXCL12 chemokine receptor CXCR4 on their basophils when compared to CT (**FIG 1C-D**). Unlike SLE patients (18, 20), CD62L expression was not significantly increased on MCTD patient basophils whereas CCR3 (the chemokine receptor mainly for eotaxin (CCL11) and CCL5) expression was dramatically increased (**FIG 1E-F**). Since CCL11-CCR3 axis is known to drive granulocyte recruitment in lungs in allergic airway inflammation and in a mouse model of lung fibrosis (25, 26), this increased CCR3 expression along with peripheral basopenia may suggest a stronger lung-oriented migration abilities of basophils in MCTD patients. A significant trend on increased expression of FcεRIα on the surface of MCTD patient basophils was also noticed (**FIG 1G**) but was not associated with significantly increased total IgE levels (**FIG 1H**) unlike what is observed in allergic or SLE patients (18, 27). The latter parameter suggested a qualitative over a quantitative serological difference concerning IgE. As expected, all MCTD patients had anti-U1 snRNP (70k) autoreactive IgG (**FIG 1I**) and nearly 80% of them had significant levels of anti-U1 snRNP (70k) autoreactive IgE (**FIG 1J** and **Table E1** in the Online Repository) (significant defined as superior to mean of CT values + 2 standard deviations).

Altogether, these results indicated that basophils were activated in MCTD patient blood during the course of the disease, as hypothesized. However, their activation pattern and the expressed levels of the chemotactic receptors CCR3 was clearly different from the profiles observed on healthy donor and SLE patient basophils, suggesting specific migration abilities of basophils during MCTD. Moreover, autoreactive IgE raised against U1-snRNP may contribute to such basophil activation profile in MCTD.

Basophils are activated and accumulate in lymph nodes and lungs in a MCTD-like mouse model

We next sought to verify whether we could identify a basophil phenotype similar to the one observed in MCTD patients (**FIG 1**) in a modified version of a MCTD-like mouse model developed by Greidinger et al. (11). This model consists of immunizing mice against a fusion protein between the maltose-binding protein (MBP) and a portion of the Human 70kDa protein of the U1-snRNP complex as previously described (see **Methods**, **FIG 2A** and (11)). The control mice (*Mcpt8*^{DTR} mice on a C57BL6/J background) were immunized against the MBP alone allowing to rule out any effect of the immunization process *per se*. All immunized mice developed antibodies to MBP (**FIG 2B**), and all U1-snRNP-MBP immunized mice developed antibodies of IgG and IgE isotypes against U1-snRNP (**FIG 2C-D**). All mice from the latter group developed cellular infiltrates in the perivascular, peribronchial and interstitial areas of the lungs (**FIG 2E** and see below) accordingly to the original model (11). Of note, no sign of SLE-like disease was observed in the MCTD-like mice as no IgG- and C3-containing immune complex deposits were observed in their kidneys nor anti-dsDNA IgG in their blood (data not shown). These data indicate that the modified protocol of the MCTD-like model led to the expected immunization against the U1-snRNP antigen with anti-U1-snRNP antibodies of IgG and IgE isotypes, and to MCTD-like lung disease development without inducing a SLE-like phenotype. This modified model was then relevant to analyze basophil contribution to the disease.

As for SLE-like mouse models (18-20), we could not recapitulate the peripheral basopenia observed in MCTD patient blood (**FIG 1A-B** and **FIG 3A**). However, blood basophils from U1-snRNP-MBP immunized mice showed a similar phenotype to the MCTD patient blood basophils with an increased activation status (CD200R expression), and increased CCR3 and CXCR4 levels (**FIG 3B-D**). Interestingly, basophils neither accumulated in the spleen of the MCTD-like mice nor in bone marrow (**FIG E2** in the Online Repository), but did accumulate in the upper lymph nodes of the mice (cervical and brachial), in broncho-alveolar lavage (BAL) and in the lung tissue (**FIG 3E-L** and **FIG E3-E5** in the Online Repository). These data suggested that basophils do not have the same behavior in this MCTD-like mouse model as compared to SLE-like mouse models where they accumulate in all secondary lymphoid organs (spleen and lymph nodes) and not in the injured organ (kidney) (18, 20). This suggested that basophils may be involved in the development of the lung pathology observed in the MCTD-like mouse model, both at the humoral level (through lymph node accumulation) and probably at the effector level through lung accumulation.

Basophils promote MCTD-like lung disease

In order to evaluate basophil contribution to the development of the lung pathology in this MCTD-like mouse model, we depleted basophils through the injection of diphtheria toxin (DT) during the last 10 days of the protocol (see **Methods and FIG 2A**). We then evaluated the lung pathology, immune cell infiltrates in the lungs and collagen and pro-inflammatory cytokines at the mRNA level. Basophil depletion was effective and specific for the basophil compartment (**FIG E4** and **E5** in the Online Repository). The basophil depletion dampened the cellular infiltrates in peribronchial, perivascular and interstitial areas (**FIG 4A-C**), demonstrating basophil contribution to this mild MCTD-like lung pathology development. As the original MCTD-like mouse model, the modified model was characterized by a marked $CD4^+$ T cell recruitment into the lungs ((6, 11), **FIG 4D** and **FIG E5F** in the Online Repository). U1-snRNP-MBP immunization and/or basophil depletion did not lead to any difference in the proportions of all other hematopoietic cell types analyzed in the lungs of the mice

(**FIG E5** in the Online Repository). Accordingly and as expected (28, 29), 10 days long basophil depletion neither reduced anti-MBP nor anti-U1snRNP antibody titers (**FIG 2A-D**) in the sustained immunization protocol followed (see **Methods, FIG 2A** and (28)). Clearly, however, basophil depletion led to a dramatic decrease in the proportions of $CD4^+$ T cells recruited to the lungs during the course of the disease (**Fig. 4D** and **FIG E5F** in the Online Repository) suggesting a central effector role of basophils for the accumulation of pathogenic CD4+ T cells in the MCTD-like lung disease development.

Next, we analyzed the expression levels of various genes of interest in mRNA extracted from the lungs of immunized mice (**FIG 4E-H and FIG E6** in the Online Repository). First, analysis of collagen I and III mRNA expressions demonstrated, as already shown at the morphology level (**FIG 2E**), that the induced lung disease at the time of sacrifice did not reach the fibrotic state as evidenced by unchanged Col3a1 mRNA levels (**FIG 4E**). However, the development of lung fibrosis was putatively initiated as increased levels of Col1a1 mRNA were detected (**FIG 4F**) along with increased IL-4 and CCL11 mRNA levels (**Fig. 4G,H**). In line with the reduced lung pathology observed in basophil-depleted MCTD-like mice (**FIG 4A-D**), basophil depletion led to normalized levels of Col1a1, IL-4 and CCL11 mRNAs (**FIG 4F-H**), strongly suggesting that basophils were required to organize the pro-TH2 and pro-fibrotic inflammatory environment in the lungs during the course of the disease. Of note, basophil depletion also reduced the pro-TH1 inflammatory environment as evidenced by the significant reduction in IFNγ mRNA levels observed in the lung of the U1-snRNP-MBP immunized mice, whereas no change in CXCL12 mRNA levels were observed in any of the analyzed conditions (**FIG E6** in the Online Repository).

Altogether, these data demonstrate that basophil depletion in the MCTD-like mouse model used dampened the measured lung pathology in terms of interstitial, peribronchial and pervivascular cellular infiltrates, $CD4^+$ T cell accumulation and pro-inflammatory and pro-fibrotic environment.

IgE deficiency prevents the activation of basophils during MCTD-like disease development

As we observed the high prevalence of autoreactive IgE both in MCTD patients and in mice developing MCTD-like lung disease, we investigated the contribution of IgE in basophil activation and localization in lungs and lymph nodes during the development of the MCTD-like lung disease. For this purpose, we immunized IgE-deficient mice (*Igh7* $^{-/-}$ (24)) with either MBP alone or U1-snRNP(70k)-MBP fusion protein and evaluated their basophil phenotype. As anticipated, IgE deficiency did not influence the proportion of blood basophils (**FIG 5A**) in the U1-snRNP70k-MBP immunized mice but completely prevented their activation (**FIG 5B**), their up-regulation of surface CCR3 and CXCR4 (**FIG 5C-D**) and their accumulation in lymph nodes (**FIG 5E**). This was accompanied by the nearly complete abrogation of basophil accumulation in the BAL of IgE-deficient mice immunized with the U1-snRNP-MBP (**FIG 5F**). These results strongly support the critical role of IgE in the activation of basophils during MCTD-like disease development enabling their migration to lymph nodes and accumulation in lungs.

IgE deficiency prevents MCTD-like lung disease development

Based on this, we next evaluated the MCTD-like lung pathology in the IgE-deficient mice (*Igh7* $^{-/-}$). Like basophil depletion (**FIG 4**), IgE deficiency similarly protected the immunized mice from developing perivascular, peribronchial or interstitial immune cell infiltrates (**FIG 6A-C**) including the accumulation of $CD4^+$ T cells in lungs (**FIG 6D**). Accordingly, no increase in Col3a1, Col1a1, IL-4 and CCL11 mRNA levels was observed in IgE-deficient mice immunized with U1-snRNP (70k)-MBP when compared to their MBP-immunized counterparts (**FIG 6E-H**). Importantly, immunization against either MBP or U1-snRNP-MBP antigens were as efficient in terms of specific IgG production in IgE-sufficient and IgE-deficient animals (**FIG E7** in the Online Repository).

Altogether, these data demonstrate that IgE deficiency prevents basophil activation, their subsequent migration to lymph nodes and lungs, and the basophil-dependent development of the MCTD-like lung disease.

DISCUSSION

Current understanding of MCTD pathophysiology is limited. Autoreactive T and B cells cooperate to drive the production of pathogenic autoantibodies and immune complexes that target endothelial cells and putatively specifically, at least in a majority of patients, the lung tissue. As for a number of autoimmune diseases, including connective tissue diseases such as SLE, MCTD patients have no specific treatment available. Thus, developing knowledge about cells and mediators involved in disease development, tissue injury and organ function loss will benefit affected patients to conceive new therapies for the studied disease. Moreover, for distinct clinical entities that share some pathophysiological processes, developing (or repurposing) innovative therapeutic modalities for one given disease may benefit also to all the related conditions.

We previously described the contribution of basophils, IgE and autoreactive IgE to the pathogenesis of SLE (18-21, 30). Our studies allowed to decipher the mechanisms by which basophils are activated and accumulate in secondary lymphoid organs in various SLE-like mouse models and more importantly in SLE patients (18-20). These studies, which were confirmed by other laboratories (31, 32), led us to test new therapeutic modalities for SLE patients and led to a phase Ib clinical trial evaluating the safety and tolerability of Omalizumab (a humanized anti-IgE monoclonal antibody) in SLE patients that showed some promising preliminary results (20, 22). Here, we demonstrate that both basophils and IgE may as well represent relevant therapeutic targets in the context of Sharp syndrome. Indeed, basophil depletion dampened lung cellular infiltrates, reduced pro-TH2 and pro-inflammatory environment and prevented fibrosis initiation in the lungs in the MCTD-like mouse model. Similarly, IgE deficiency completely prevented disease development. In that perspective, the present study identifies both basophils and IgE as new therapeutic targets in MCTD.

The prevalence of autoreactive anti-U1-snRNP (70) IgE in our cohort was around 80%. The analysis of a larger number of patients in the coming years will allow to determine a more precise prevalence of

such autoreactive IgE and whether other autoantigen specificities for IgE can be detected in MCTD patients.

Basophil depletion in our study was achieved by using the *Mcpt8*^{DTR} mice on the C57BL/6J genetic background developed by Wada et al. (23). Recently, El Hachem *et al.* nicely reported that injections of a similar dose of DT was inducing granulocyte-macrophage progenitor depletion in the bone marrow of *Mcpt8*^{DTR} mice on the Balb/c genetic background, resulting in a depletion of eosinophils and neutrophils (33). In our set up, 250 ng of DT per injection could not achieve more than a 50% depletion of basophils (*data not shown*). The use of 1 µg DT per injection was mandatory to achieve basophil complete depletion and did not lead to the depletion of eosinophils or neutrophils in all the analyzed compartments (**FIG E4** and **E5** in the Online Repository). This is more than likely due to a difference in the bioactivity of the unnicked DT used and/or to the different genetic backgrounds of the mice.

The MCTD-mouse model used here, adapted from the original model developed by Greidinger et al. (11), involves an immunization with complete Freund adjuvant followed by a boost in incomplete Freund adjuvant. Thus, the present study could not evaluate the early immunoregulatory role of basophils in the production of autoreactive antibodies and in its amplification as we did in the SLE context (18, 20). Indeed, basophil depletion did not impact the titers of anti-U1-snRNP antibodies in immunized mice (**FIG 2**) as expected since basophils are not required for CFA-induced antigen sensitization *in vivo* (28). However, based on our previous studies and on the phenotype of MCTD patient basophils (CXCR4 increased expression), these cells, by accumulating in lymph nodes, may support autoantibody production as they do in SLE. A spontaneous MCTD-like mouse model is still lacking to the field to decipher further the first steps of the MCTD pathophysiology. Another limitation of the MCTD-like mouse model used in our study is the time chosen for analysis. On one hand, it allowed describing the high relevance of basophil effector function in the primary inflammatory processes of the lung disease development. On the other hand, later time points of the

disease should be analyzed as well, once the lung fibrosis is well established and basophil contribution to such late phases should be addressed. Indeed, interstitial lung disease in patients is often diagnosed once it is well established and rarely at the very early phases. Thus, evaluating basophil depletion as a putative therapeutic approach in lungs more impacted by fibrosis may be of interest for translation to human therapeutics.

Targeting directly basophils may then be of clinical interest in MCTD and SLE as suggested by our results. A therapy targeting specifically basophils at the cellular level is not, to our knowledge, currently available. However, a promising anti-CD123 (the IL-3 receptor α chain) monoclonal antibody, CSL362, allows targeting key cells in CTD pathogenesis which are plasmacytoid dendritic cells and basophils (18, 20, 31, 34, 35). Interestingly, the anti-CD123 targeted cells are the same as the one activated by autoreactive IgE in SLE and MCTD (18, 31, 32).

Concerning the mechanistic understanding of MCTD lung pathology, our report provides some new parameters to take into accounts in further studies. The most striking marker differentially expressed on MCTD patient basophils was CCR3, suggesting an involvement of basophil, CCR3 and its main ligand CCL11 in the course of the disease and this was recapitulated in the MCTD-like mouse model. Despite the fact that the lung pathology at the time of analysis was really mild, we could detect collagen I mRNA accumulation in lungs of U1-snRNP immunized mice suggesting the early development of lung fibrosis. This parameter was clearly associated with the detection of IL-4 and CCL11 mRNA in the same lung extracts. Strikingly, basophil depletion or IgE deficiency completely normalized such pathological parameters and also dampened CD4+ T cells recruitment to the lungs. CCL11 in the lungs is induced by IL-4 and allows recruitment of CCR3 bearing cells in the bleomycin-induced mouse model of lung fibrosis (26, 36). Recently, basophil-derived IL-4 was shown to promote emphysema in a mouse model of elastase-induced chronic obstructive pulmonary disease (COPD) (16). Then, one working hypothesis could be that basophils, activated through anti-U1-snRNP antibodies in a complex with their autoantigen, and overexpressing CCR3 would tend to accumulate

in airways and lung tissue. Once recruited, their IL-4 production may upregulate CCL11 levels in the airways, leading to both recruitment of CCR3 expressing $CD4^+$ TH2 cells and to the maintenance of IL-4 pressure to amplify TH2 differentiation. Such an amplification loop of the pro-fibrotic TH2 environment in the lungs may then facilitate and induce long-term development of lung fibrosis. In this scenario, basophils may then play both effector and immunoregulatory roles in the pathophysiology of MCTD lung disease development.

IgE deficiency completely prevented basophil activation and accumulation both in lymph nodes and lungs, suggesting that the role of basophils depends on IgE-mediated activation in the MCTD pathogenesis. A spontaneous mouse model of MCTD will be required to determine whether basophils are as well involved in the generation or the amplification of such autoreactive IgE and IgG productions and contribute to an amplification loop of the disease as they do in SLE.

Our study identifies the basophil/IgE/IL-4/CCL11 axis as a relevant candidate for further investigations aiming to define specific therapeutic approaches for lung involvement in Sharp Syndrome. For instance, antagonizing CCR3 and CCL11 interaction may be a valuable approach to prevent basophil accumulation in lungs and their deleterious effects. This approach should be selectively appreciated in MCTD and probably not in SLE, since in the latter condition, we could not detect any variation of CCR3 expression by basophils (20).

As suggested by our present report, targeting IgE to prevent the actions of autoreactive IgE may resume the beneficial effects that we observed on lung pathology in the context of IgE deficiency. As for SLE, Omalizumab may be a reasonable, safe and effective approach (22) along with other IgE targeting monoclonal antibodies such as ligelizumab and UB-221 that are currently under clinical development for treatment of chronic spontaneous urticaria, another autoimmune condition dependent on autoreactive IgE (37).

AUTHOR CONTRIBUTIONS

Y.L. designed and conducted experiments and wrote the manuscript. S.V., E.P. and F.S. conducted experiments. E.B. designed all the constructs and produced all the recombinant proteins used in the study. A.M. participated in establishing the lung pathology scores and edited the manuscript. U.B. and M.B. were involved in the project development and edited the manuscript. K.S., B.C., T.P. and E.D. recruited patients, provided clinical data and edited the manuscript. K.S. analyzed clinical data of the cohort, provided pre-clinical analysis and edited the manuscript. N.C. conceived and directed the project, designed experiments, conducted experiments and wrote the manuscript.

ACKNOWLEDGMENTS

The authors wish to acknowledge the nurses and clinicians from Bichat hospital's Internal Medicine, Nephrology and Pulmonology departments and all the members of the Centre de Recherche sur l'Inflammation for their invaluable help. We thank Pr Hajime Karasuyama from the Department of Immune Regulation, Graduate School of Medical and Dental Sciences, Tokyo Medical and Dental University (TMDU), Tokyo 113-8510, Japan, for providing the *Mcpt8*^{DTR} mice. We also thank Prof. Hans Oettgen (Harvard Medical School, Boston, MA, USA) and Dr Juan Rivera (National Institute of Arthritis, Musculoskeletal and Skin diseases (NIAMS), NIH, Bethesda, MD, USA) for generating and providing the *Igh7*$^{-/-}$ mice, respectively. We are indebted to the colleagues from animal care, flow cytometry and morphology core facilities of the Bichat School of Medicine.

ADDITIONAL INFORMATION

CONFLICT OF INTEREST STATEMENT: The authors declare that they have no relevant conflict of interest.

ONLINE REPOSITORY: Seven supplementary figures (FIG E1 to E7) and two supplementary tables (Tables E1 and E2).

REFERENCES

1. Sharp GC, Irvin WS, Tan EM, Gould RG, Holman HR. Mixed connective tissue disease--an apparently distinct rheumatic disease syndrome associated with a specific antibody to an extractable nuclear antigen (ENA). Am J Med. 1972;52(2):148-59.
2. Ungprasert P, Crowson CS, Chowdhary VR, Ernste FC, Moder KG, Matteson EL. Epidemiology of Mixed Connective Tissue Disease, 1985-2014: A Population-Based Study. Arthritis Care Res (Hoboken). 2016;68(12):1843-8.
3. Venables PJ. Mixed connective tissue disease. Lupus. 2006;15(3):132-7.
4. Sapkota B, Al Khalili Y. Mixed Connective Tissue Disease. StatPearls. Treasure Island (FL)2020.
5. Hof D, Cheung K, de Rooij DJ, van den Hoogen FH, Pruijn GJ, van Venrooij WJ, et al. Autoantibodies specific for apoptotic U1-70K are superior serological markers for mixed connective tissue disease. Arthritis Res Ther. 2005;7(2):R302-9.
6. Greidinger EL, Zang YJ, Jaimes K, Martinez L, Nassiri M, Hoffman RW. CD4+ T cells target epitopes residing within the RNA-binding domain of the U1-70-kDa small nuclear ribonucleoprotein autoantigen and have restricted TCR diversity in an HLA-DR4-transgenic murine model of mixed connective tissue disease. J Immunol. 2008;180(12):8444-54.
7. Enomoto K, Takada T, Suzuki E, Ishida T, Moriyama H, Ooi H, et al. Bronchoalveolar lavage fluid cells in mixed connective tissue disease. Respirology. 2003;8(2):149-56.
8. Paradowska-Gorycka A. U1-RNP and TLR receptors in the pathogenesis of mixed connective tissue diseasePart I. The U1-RNP complex and its biological significance in the pathogenesis of mixed connective tissue disease. Reumatologia. 2015;53(2):94-100.
9. Greidinger EL, Foecking MF, Magee J, Wilson L, Ranatunga S, Ortmann RA, et al. A major B cell epitope present on the apoptotic but not the intact form of the U1-70-kDa ribonucleoprotein autoantigen. J Immunol. 2004;172(1):709-16.
10. Okawa-Takatsuji M, Aotsuka S, Uwatoko S, Takaono M, Iwasaki K, Kinoshita M, et al. Endothelial cell-binding activity of anti-U1-ribonucleoprotein antibodies in patients with connective tissue diseases. Clin Exp Immunol. 2001;126(2):345-54.
11. Greidinger EL, Zang Y, Jaimes K, Hogenmiller S, Nassiri M, Bejarano P, et al. A murine model of mixed connective tissue disease induced with U1 small nuclear RNP autoantigen. Arthritis Rheum. 2006;54(2):661-9.
12. Dema B, Charles N. Advances in mechanisms of systemic lupus erythematosus. Discovery medicine. 2014;17(95):247-55.
13. Kaul A, Gordon C, Crow MK, Touma Z, Urowitz MB, van Vollenhoven R, et al. Systemic lupus erythematosus. Nat Rev Dis Primers. 2016;2:16039.
14. Fanouriakis A, Kostopoulou M, Alunno A, Aringer M, Bajema I, Boletis JN, et al. 2019 update of the EULAR recommendations for the management of systemic lupus erythematosus. Ann Rheum Dis. 2019;78(6):736-45.
15. Hussain M, Borcard L, Walsh KP, Pena Rodriguez M, Mueller C, Kim BS, et al. Basophil-derived IL-4 promotes epicutaneous antigen sensitization concomitant with the development of food allergy. J Allergy Clin Immunol. 2018;141(1):223-34 e5.
16. Shibata S, Miyake K, Tateishi T, Yoshikawa S, Yamanishi Y, Miyazaki Y, et al. Basophils trigger emphysema development in a murine model of COPD through IL-4-mediated generation of MMP-12-producing macrophages. Proc Natl Acad Sci U S A. 2018;115(51):13057-62.
17. Yamanishi Y, Karasuyama H. Basophil-derived IL-4 plays versatile roles in immunity. Semin Immunopathol. 2016;38(5):615-22.
18. Charles N, Hardwick D, Daugas E, Illei GG, Rivera J. Basophils and the T helper 2 environment can promote the development of lupus nephritis. Nature medicine. 2010;16(6):701-7.
19. Dema B, Lamri Y, Pellefigues C, Pacreau E, Saidoune F, Bidault C, et al. Basophils contribute to pristane-induced Lupus-like nephritis model. Sci Rep. 2017;7(1):7969.

20. Pellefigues C, Dema B, Lamri Y, Saidoune F, Chavarot N, Loheac C, et al. Prostaglandin D2 amplifies lupus disease through basophil accumulation in lymphoid organs. Nat Commun. 2018;9(1):725.
21. Dema B, Charles N, Pellefigues C, Ricks TK, Suzuki R, Jiang C, et al. Immunoglobulin E plays an immunoregulatory role in lupus. The Journal of experimental medicine. 2014;211(11):2159-68.
22. Hasni S, Gupta S, Davis M, Poncio E, Temesgen-Oyelakin Y, Joyal E, et al. Safety and Tolerability of Omalizumab: A Randomized Clinical Trial of Humanized Anti-IgE Monoclonal Antibody in Systemic Lupus Erythematosus. Arthritis Rheumatol. 2019;71(7):1135-40.
23. Wada T, Ishiwata K, Koseki H, Ishikura T, Ugajin T, Ohnuma N, et al. Selective ablation of basophils in mice reveals their nonredundant role in acquired immunity against ticks. J Clin Invest. 2010;120(8):2867-75.
24. Oettgen HC, Martin TR, Wynshaw-Boris A, Deng C, Drazen JM, Leder P. Active anaphylaxis in IgE-deficient mice. Nature. 1994;370(6488):367-70.
25. Deppong CM, Green JM. Experimental advances in understanding allergic airway inflammation. Front Biosci (Schol Ed). 2013;5:167-80.
26. Huaux F, Gharaee-Kermani M, Liu T, Morel V, McGarry B, Ullenbruch M, et al. Role of Eotaxin-1 (CCL11) and CC chemokine receptor 3 (CCR3) in bleomycin-induced lung injury and fibrosis. Am J Pathol. 2005;167(6):1485-96.
27. Berings M, Gevaert P, De Ruyck N, Derycke L, Holtappels G, Pilette C, et al. FcepsilonRI expression and IgE binding by dendritic cells and basophils in allergic rhinitis and upon allergen immunotherapy. Clin Exp Allergy. 2018;48(8):970-80.
28. Ishida W, Fukuda K, Sumi T, Ebihara N, Kajisako M, Matsuda H, et al. Adjuvants determine the contribution of basophils to antigen sensitization in vivo. Immunol Lett. 2011;136(1):49-54.
29. Otsuka A, Nakajima S, Kubo M, Egawa G, Honda T, Kitoh A, et al. Basophils are required for the induction of Th2 immunity to haptens and peptide antigens. Nat Commun. 2013;4:1739.
30. Dema B, Pellefigues C, Hasni S, Gault N, Jiang C, Ricks TK, et al. Autoreactive IgE is prevalent in systemic lupus erythematosus and is associated with increased disease activity and nephritis. PLoS One. 2014;9(2):e90424.
31. Henault J, Riggs JM, Karnell JL, Liarski VM, Li J, Shirinian L, et al. Self-reactive IgE exacerbates interferon responses associated with autoimmunity. Nat Immunol. 2016;17(2):196-203.
32. Pan Q, Gong L, Xiao H, Feng Y, Li L, Deng Z, et al. Basophil Activation-Dependent Autoantibody and Interleukin-17 Production Exacerbate Systemic Lupus Erythematosus. Front Immunol. 2017;8:348.
33. El Hachem C, Hener P, Kirstetter P, Li J, Chan S, Li M. Treatment of MCPT8(DTR) mice with high- or low-dose diphtheria toxin leads to differential depletion of basophils and granulocyte-macrophage progenitors. Eur J Immunol. 2018;48(5):861-73.
34. Oon S, Huynh H, Tai TY, Ng M, Monaghan K, Biondo M, et al. A cytotoxic anti-IL-3Ralpha antibody targets key cells and cytokines implicated in systemic lupus erythematosus. JCI Insight. 2016;1(6):e86131.
35. Oon S, Monaghan K, Ng M, Hoi A, Morand E, Vairo G, et al. A potential association between IL-3 and type I and III interferons in systemic lupus erythematosus. Clin Transl Immunology. 2019;8(12):e01097.
36. Hosokawa Y, Hosokawa I, Shindo S, Ozaki K, Matsuo T. IL-4 Modulates CCL11 and CCL20 Productions from IL-1beta-Stimulated Human Periodontal Ligament Cells. Cell Physiol Biochem. 2016;38(1):153-9.
37. Kolkhir P, Altrichter S, Munoz M, Hawro T, Maurer M. New treatments for chronic urticaria. Ann Allergy Asthma Immunol. 2020;124(1):2-12.

FIGURE LEGENDS

Figure 1: MCTD patients have activated basophils and autoreactive IgE raised against U1-snRNP

(**A-B**) Proportion (**A**) and absolute number (**B**) of basophils among leukocytes determined by flow cytometry as described in the **Methods** section and **FIG E1A** (in the Online Repository) in the blood of healthy donors (CT, n=32), MCTD patients and (MCTD, n=16) as described in **Table E1** (in the Online Repository). (**C-G**), Surface expression levels of CD203c (**C**), CXCR4 (**D**), CD62L (**E**), CCR3 (**F**) and FcεRIα (**G**) were quantified by flow cytometry. Data are expressed as the ratio of the geometric mean of fluorescence intensity (gMFI) of the specific marker on the gMFI of the isotype control restricted to the FSC/SSC gate corresponding to basophils and expressed in arbitrary units (A.U.). (**H**) Quantitation of total serum IgE levels in healthy controls and MCTD patients by ELISA. (**I**-**J**) IgG (**I**) and IgE (**J**) anti-U1-snRNP (70k) was determined by semi-quantitative ELISA (as described in the **methods**). (**A**-**J**) Data are expressed as median and interquartile ranges with whiskers representing 5-95 percentiles and the mean presented as a '+' symbol. Statistical analyses were by Mann-Whitney *U* tests. NS: not significant; **: p<0.01; ***: p<0.001; ****: p<0.0001.

Figure 2: U1-snRNP-MBP immunization induces inflammatory infiltrates in lungs, and the development of IgG and IgE anti-U1-snRNP 70k.

(**A**) Schematic of the MCTD-like mouse model and the DT-mediated basophil depletion protocols (See **Methods** for further details). sc: subcutaneously; Complete Freund Adjuvant (CFA); Incomplete Freund adjuvant (IFA). For basophil depletion experiments, C57BL/6J *Mcpt8*^{DTR} mice received four intraperitoneal injections (red arrows) of 1 µg of diphteria toxin (DT) or vehicle in 100 µL of PBS 10, 9, 4 and 1 days before sacrifice. (**B**,**C**,**D**) Quantification by ELISA of serum IgG antibodies raised against MBP (**B**) and U1-snRNP (**C**) and IgE antibodies raised against U1-snRNP (**C**) in *Mcpt8*^{DTR} mice immunized with MBP alone (M) or with U1-snRNP-MBP (70k) and basophil-depleted (Diphtheria toxin (DT) +) or not (DT–) over the 10 last days of the protocol. (M DT–: n= 8; M DT+: n= 9; 70k DT–:

n= 16; 70k DT+: n=11). Data are expressed as the mean + s.e.m. of optical density at 405 nm normalized to the mean of the control values (M DT– mice) for the concerned antigen. Statistical analysis was done by one-way analysis of variance (ANOVA) followed by unpaired Student *t* test between the indicated groups. (**E**) After 6 weeks of immunization protocol (see **Methods**), mice were sacrificed, lungs harvested, fixed in formalin 10% and included in paraffin. 5 µm sections were stained by Masson's trichrome. A score of the pathology was designed to quantify inflammatory cell infiltrations in the interstitial, peribronchial and perivascular areas of the lungs (see **Methods**). Scale bar: 200 µm.

Figure 3: Basophils are activated and accumulate in lymph nodes and lungs during MCTD-like disease development

(**A**-**L**) Flow cytometry analysis of the basophil compartment (defined as $CD19^-$ $TCR\beta^-$ $CD117^-$ $CD49b^+$ and brachial) (**E**-**H**) and bronchoalveolar lavage (BAL) (**I**-**L**) from mice immunized with MBP alone (M) (blood and LN: n=15; BAL: n=11) or with U1-snRNP-MBP (70k) (blood and LN: n=27; BAL: n=14). (**A**,**E**,**I**) Proportion of basophils among $CD45^+$ cells in the indicated compartments. Surface expression levels of CD200R (**B**,**F**,**J**), CCR3 (**C**,**G**,**K**) and CXCR4 (**D**,**H**,**L**) were quantified by flow cytometry. (**B**-**D**, **F**-**H**, **J**-**L**) Data are expressed as the ratio of the geometric mean of fluorescence intensity (gMFI) of the specific marker on the gMFI of the isotype control restricted to the FSC/SSC gate corresponding to basophils and expressed in arbitrary units (A.U.). (**A**-**L**) Data are expressed as mean + s.e.m.. Statistical analyses were done by unpaired Student *t* test. NS: not significant; *: p<0.05; **: p<0.01; ***: p<0.001; ****: p<0.0001.

Figure 4: Basophils contribute to MCTD-like lung disease development

(**A**-**C**) A score of the lung pathology was designed to quantify inflammatory cell infiltrations in the perivascular (**A**), peribronchial (**B**) and interstitial (**C**) areas of the lungs (see **Methods**). Lung pathology score was determined in *Mcpt8*^{DTR} mice immunized with MBP alone (M) or with MBP-U1-snRNP (70k) basophil depleted (Diphtheria toxin (DT) +) or not (DT–) over the 10 last days of the protocol. (M DT–: n= 5; M DT+: n= 5; 70k DT–: n= 6; 70k DT+: n=6). (**D**) Proportion of $CD4^+$ T cells (defined as $CD45^+$ $CD19^-$ $CD117^-$ $CD3^+$ $CD4^+$) among living $CD45^+$ cells in BAL of mice treated as described in (**A**) (M DT–: n= 8; M DT+: n= 4; 70k DT–: n= 9; 70k DT+: n=6), as determined by flow cytometry. (**E**-**H**) mRNA expression levels of the indicated targets quantified by RT-qPCR on mRNA purified from lung extracts from mice treated as described in (**A**) (M DT–: n= 13; M DT+: n= 6; 70k DT–: n= 22; 70k DT+: n=16). Data are expressed as the mean + s.e.m. of the $2^{-\Delta Ct}$ relative to the β-actin Ct. (**A**-**H**) Statistical analyses were done by one-way analysis of variance (ANOVA) followed by unpaired Student *t* test between the indicated groups. NS: not significant; *: p<0.05; **: p<0.01; ***: p<0.001; ****: p<0.0001.

Figure 5: IgE deficiency abrogates basophil activation and accumulation in lymph nodes and lungs during MCTD-like disease model

(**B**–**D**) Surface expression levels of CD200R (**B**), CXCR4 (**C**) and CCR3 (**D**) on blood basophils were quantified by flow cytometry. (**E**,**F**) Proportion of basophils among CD45+ cells in lymph nodes (cervical and brachial) (**E**) and bronchoalveolar lavage (BAL) (**F**), from WT mice immunized with MBP alone (M) (n= 11-14) or U1-snRNP-MBP (70k) (n= 14-26) and from *Igh7* $^{-/-}$ mice immunized with MBP alone (M) (n= 3) or U1-snRNP-MBP (70k) (n= 4). (**B**–**D**) Data are expressed as the ratio of the geometric mean of fluorescence intensity (gMFI) of the specific marker on the gMFI of the isotype control restricted to the FSC/SSC gate corresponding to basophils and expressed in arbitrary units (A.U.). (**A**–**F**) Data are expressed as mean ± s.e.m.. Statistical analyses were done by one-way analysis

of variance (ANOVA) followed by unpaired Student *t* test between the indicated groups. NS: not significant; *: p<0.05; **: p<0.01; ***: p<0.001; ****: p<0.0001.

Figure 6. IgE deficiency prevents MCTD-like lung disease development

(**A**-**C**) Score of the lung pathology was assessed in the perivascular (**A**), peribronchial (**B**) and interstitial (**C**) areas of the lungs (see **Methods** and **FIG 2**) in control (WT) or deficient in IgE (*Igh7*$^{-/-}$) mice immunized with MBP alone (M) or with MBP-U1-snRNP (70k). (WT M: n= 8; WT 70k: n= 9; *Igh7*$^{-/-}$ M: n=3; *Igh7*$^{-/-}$ 70k: n=4). (**D**) Proportion of CD4^{+} T cells (defined as CD45^{+} CD19^{-} CD117^{-} CD3^{+} CD4^{+}) among living CD45^{+} cells in BAL of mice treated as described in (**A**) (WT M: n= 8; WT 70k : n= 9; *Igh7*$^{-/-}$ M: n=3; *Igh7*$^{-/-}$ 70k : n=4) as determined by flow cytometry. (**E**-**H**) mRNA expression levels of the indicated targets quantified by RT-qPCR on mRNA purified from lung extracts from mice treated as described in (**A**) (WT M: n= 13; WT 70k: n= 20; *Igh7*$^{-/-}$ M: n=3; *Igh7*$^{-/-}$ 70k: n=3). Data are expressed as the mean ± s.e.m. of the $2^{-\Delta Ct}$ relative to the actin Ct. (**A**-**D**) Statistical analysis was done by one-way analysis of variance (ANOVA) followed by unpaired Student *t* test between the indicated groups. (**E**-**H**) Statistical analysis was done by Kruskal-Wallis test followed by unpaired Mann Whitney *U* test between the indicated groups. NS: not significant; *: p<0.05; **: p<0.01;***: p<0.001; ****: p<0.0001.

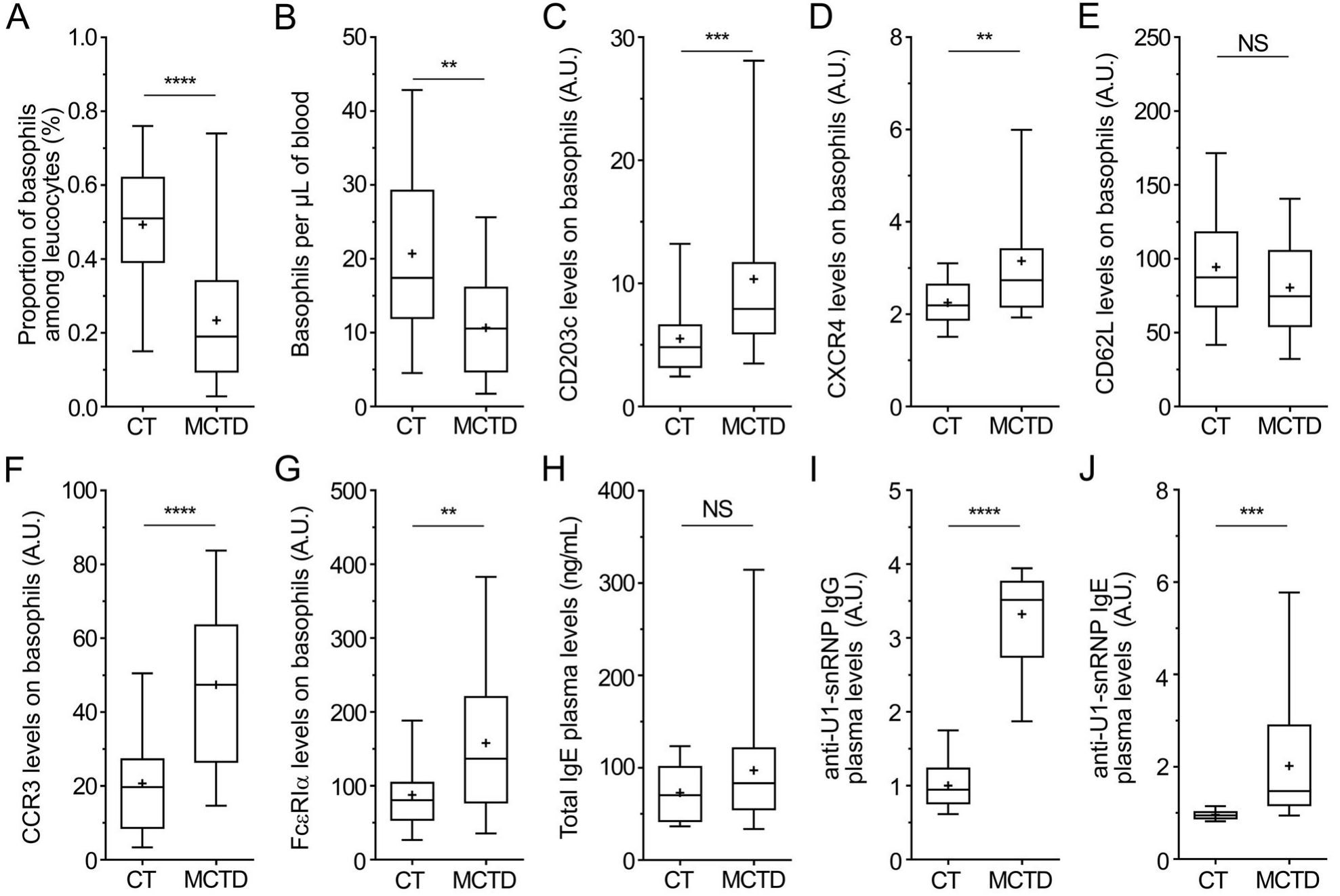
A
Proportion of basophils among leucocytes (%)
1.0
0.8
0.6
0.4
0.2
0.0
****
CT
MCTD
B
Basophils per µL of blood
50
40
30
20
10
0
**
CT
MCTD
C
CD203c levels on basophils (A.U.)
30
20
10
0
***
CT
MCTD
D
CXCR4 levels on basophils (A.U.)
8
6
4
2
0
**
CT
MCTD
E
CD62L levels on basophils (A.U.)
250
200
150
100
50
0
NS
CT
MCTD
F
CCR3 levels on basophils (A.U.)
100
80
60
40
20
0
****
CT
MCTD
G
FcεRIα levels on basophils (A.U.)
500
400
300
200
100
0
**
CT
MCTD
H
Total IgE plasma levels (ng/mL)
400
300
200
100
0
NS
CT
MCTD
I
anti-U1-snRNP IgG plasma levels (A.U.)
5
4
3
2
1
0
****
CT
MCTD
J
anti-U1-snRNP IgE plasma levels (A.U.)
8
6
4
2
0
***
CT
MCTD

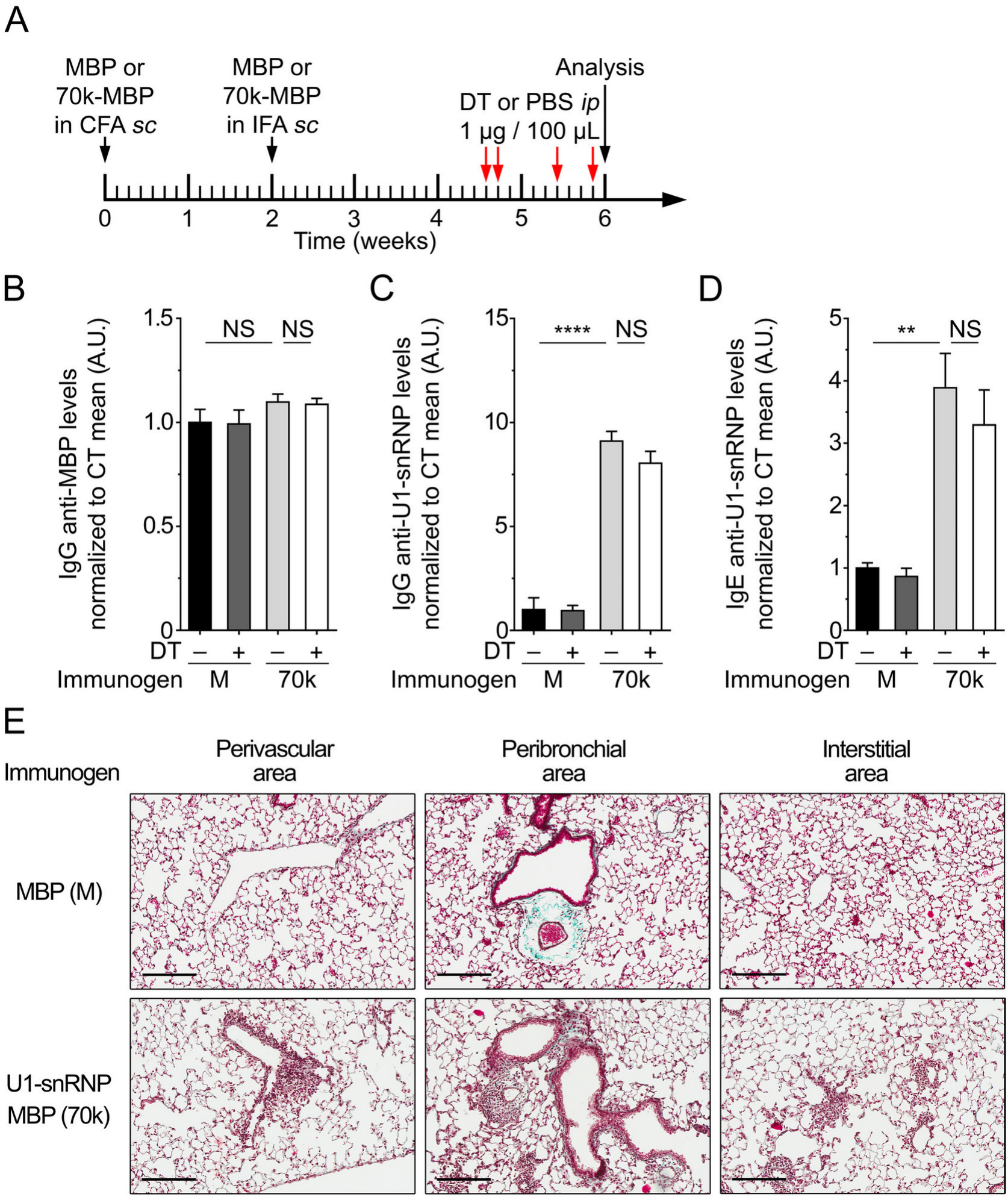
A
MBP or
70k-MBP
in CFA sc
MBP or
70k-MBP
in IFA sc
Analysis
DT or PBS ip
1 µg / 100 µL
0
1
2
3
4
5
6
Time (weeks)
B
IgG anti-MBP levels
normalized to CT mean (A.U.)
1.5
1.0
0.5
0
NS
NS
DT
–
+
–
+
Immunogen
M
70k
C
IgG anti-U1-snRNP levels
normalized to CT mean (A.U.)
15
10
5
0
****
NS
DT
–
+
–
+
Immunogen
M
70k
D
IgE anti-U1-snRNP levels
normalized to CT mean (A.U.)
5
4
3
2
1
0
**
NS
DT
–
+
–
+
Immunogen
M
70k
E
Immunogen
Perivascular
area
Peribronchial
area
Interstitial
area
MBP (M)
U1-snRNP
MBP (70k)

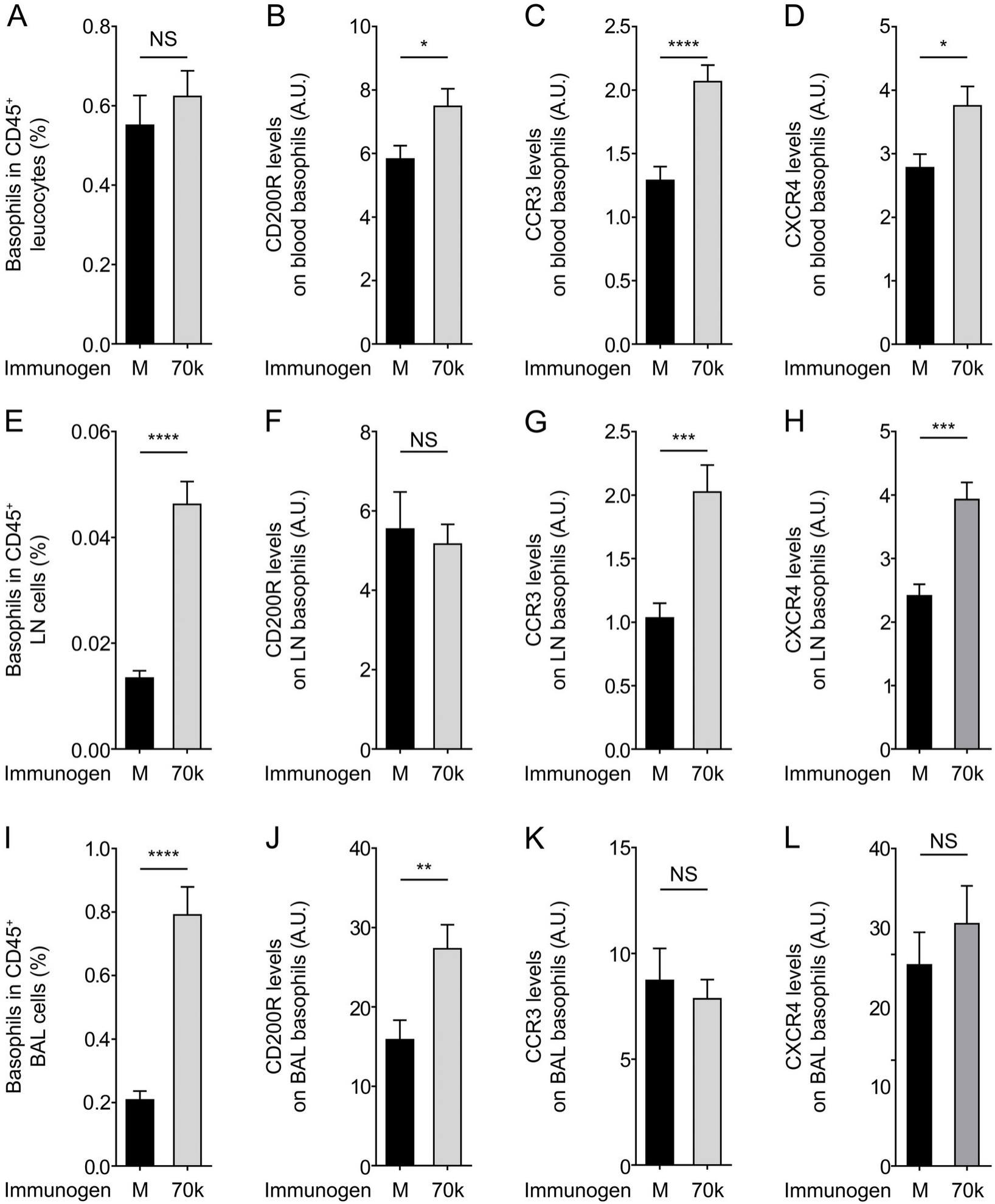
A
Basophils in CD45+ leucocytes (%)
0.8
0.6
0.4
0.2
0.0
NS
Immunogen M 70k
B
CD200R levels on blood basophils (A.U.)
10
8
6
4
2
0
*
Immunogen M 70k
C
CCR3 levels on blood basophils (A.U.)
2.5
2.0
1.5
1.0
0.5
0.0
****
Immunogen M 70k
D
CXCR4 levels on blood basophils (A.U.)
5
4
3
2
1
0
*
Immunogen M 70k
E
Basophils in CD45+ LN cells (%)
0.06
0.04
0.02
0.00
****
Immunogen M 70k
F
CD200R levels on LN basophils (A.U.)
8
6
4
2
0
NS
Immunogen M 70k
G
CCR3 levels on LN basophils (A.U.)
2.5
2.0
1.5
1.0
0.5
0.0
***
Immunogen M 70k
H
CXCR4 levels on LN basophils (A.U.)
5
4
3
2
1
0
***
Immunogen M 70k
I
Basophils in CD45+ BAL cells (%)
1.0
0.8
0.6
0.4
0.2
0.0
****
Immunogen M 70k
J
CD200R levels on BAL basophils (A.U.)
40
30
20
10
0
**
Immunogen M 70k
K
CCR3 levels on BAL basophils (A.U.)
15
10
5
0
NS
Immunogen M 70k
L
CXCR4 levels on BAL basophils (A.U.)
40
30
20
10
0
NS
Immunogen M 70k

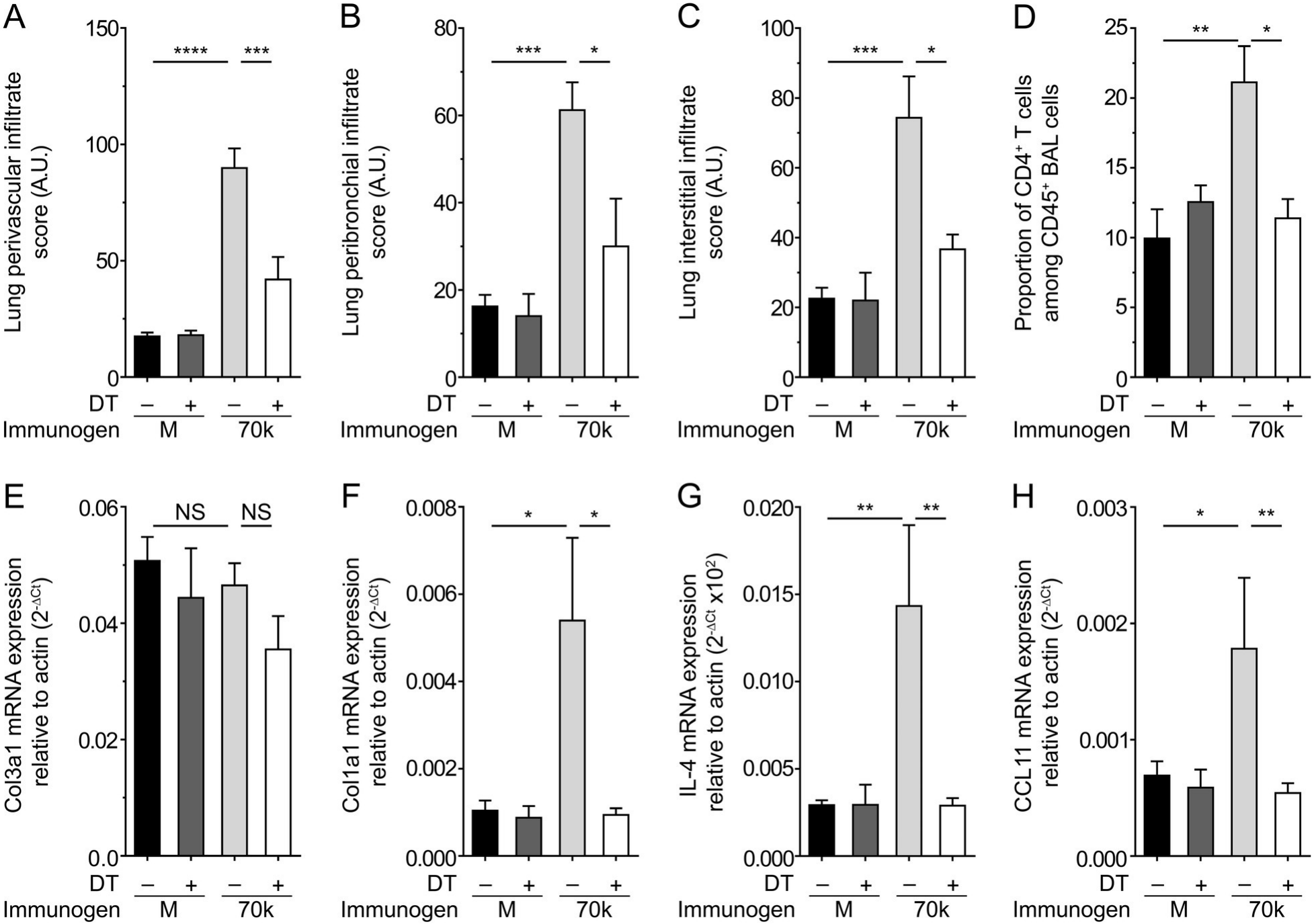
A
Lung perivascular infiltrate score (A.U.)
150
100
50
0
****
***
B
Lung peribronchial infiltrate score (A.U.)
80
60
40
20
0
***
*
C
Lung interstitial infiltrate score (A.U.)
100
80
60
40
20
0
***
*
D
Proportion of CD4+ T cells among CD45+ BAL cells
25
20
15
10
5
0
**
*
DT – + – +
Immunogen M 70k
E
Col3a1 mRNA expression relative to actin (2-ΔCt)
0.06
0.04
0.02
0.0
NS
NS
F
Col1a1 mRNA expression relative to actin (2-ΔCt)
0.008
0.006
0.004
0.002
0.000
*
*
G
IL-4 mRNA expression relative to actin (2-ΔCt x10²)
0.020
0.015
0.010
0.005
0.000
**
**
H
CCL11 mRNA expression relative to actin (2-ΔCt)
0.003
0.002
0.001
0.000
*
**

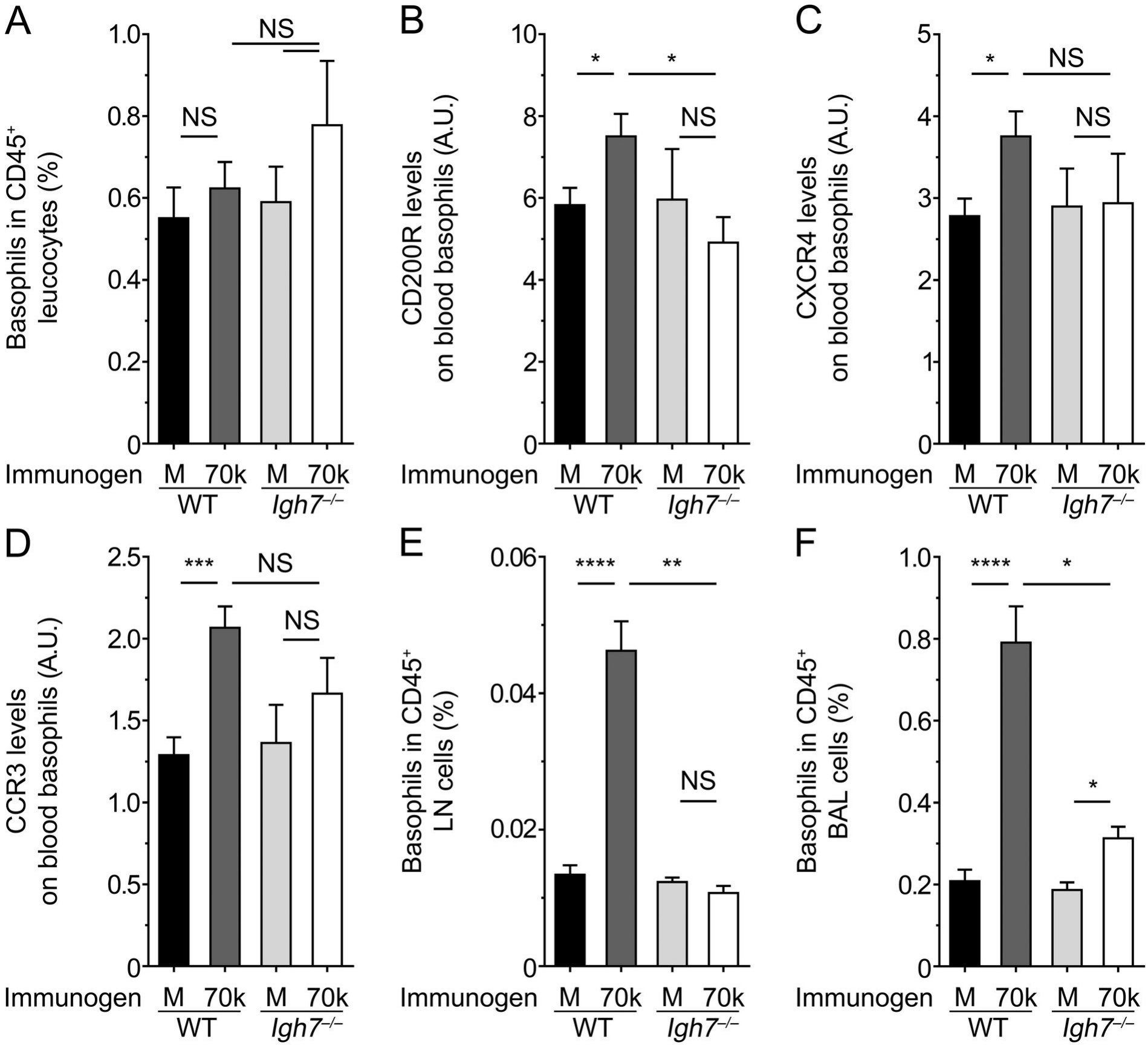
A
Basophils in CD45+ leucocytes (%)
1.0
0.8
0.6
0.4
0.2
0
NS
NS
B
CD200R levels on blood basophils (A.U.)
10
8
6
4
2
0
*
*
NS
C
CXCR4 levels on blood basophils (A.U.)
5
4
3
2
1
0
*
NS
NS
Immunogen
M 70k M 70k
WT
Igh7−/−
D
CCR3 levels on blood basophils (A.U.)
2.5
2.0
1.5
1.0
0.5
0
***
NS
NS
E
Basophils in CD45+ LN cells (%)
0.06
0.04
0.02
0
****
**
NS
F
Basophils in CD45+ BAL cells (%)
1.0
0.8
0.6
0.4
0.2
0
****
*
*

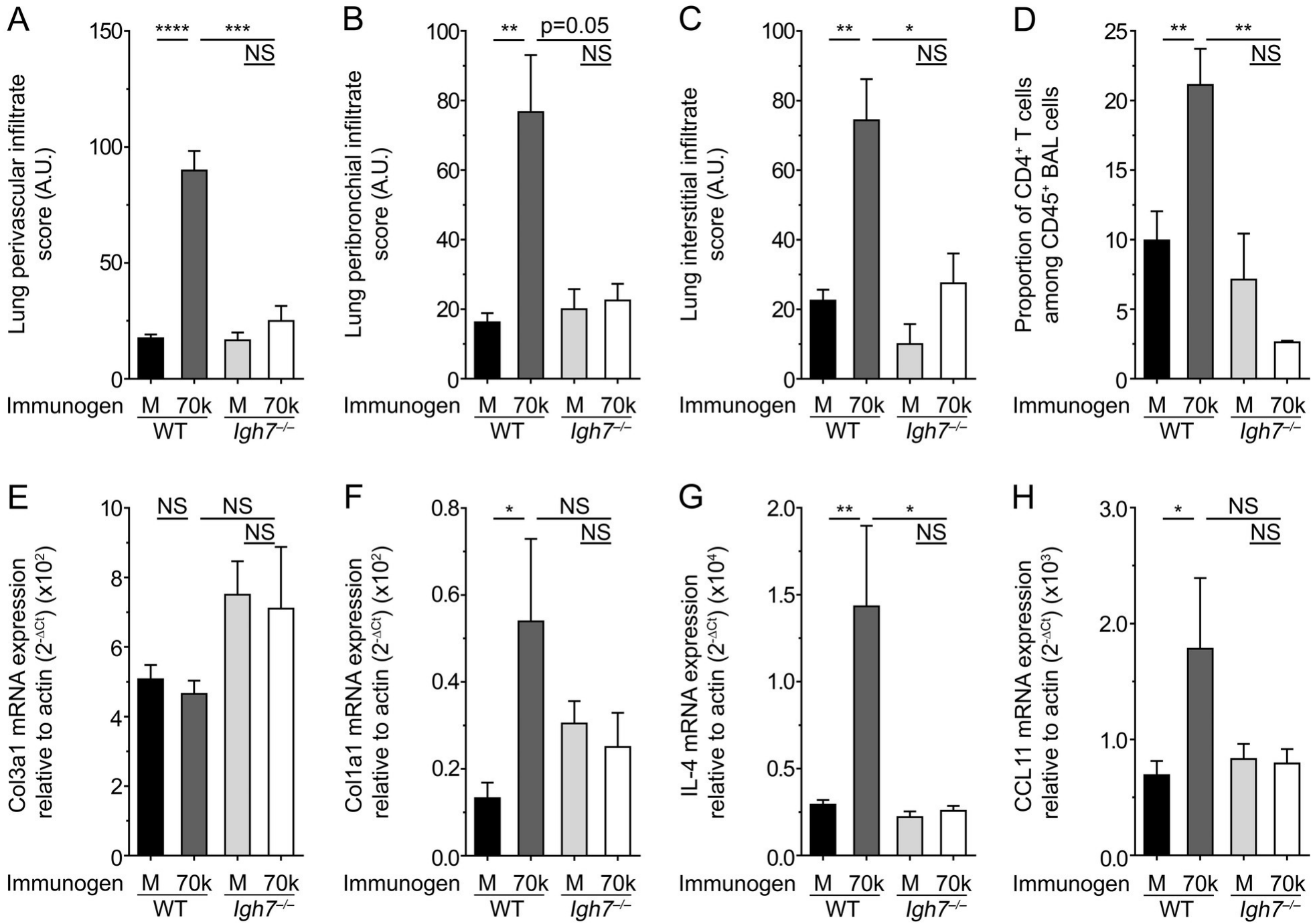
A
Lung perivascular infiltrate score (A.U.)
150
100
50
0
****
***
NS
B
Lung peribronchial infiltrate score (A.U.)
100
80
60
40
20
0
**
p=0.05
NS
C
Lung interstitial infiltrate score (A.U.)
100
80
60
40
20
0
**
*
NS
D
Proportion of CD4+ T cells among CD45+ BAL cells
25
20
15
10
5
0
**
**
NS
Immunogen
M
70k
M
70k
WT
Igh7−/−
E
Col3a1 mRNA expression relative to actin (2-ΔCt) (x10²)
10
8
6
4
2
0
NS
NS
NS
F
Col1a1 mRNA expression relative to actin (2-ΔCt) (x10²)
0.8
0.6
0.4
0.2
0.0
*
NS
NS
G
IL-4 mRNA expression relative to actin (2-ΔCt) (x10⁴)
2.0
1.5
1.0
0.5
0.0
**
*
NS
H
CCL11 mRNA expression relative to actin (2-ΔCt) (x10³)
3.0
2.0
1.0
0.0
*
NS
NS